Use of Rhodamine-allyl Schiff base by chemodosimetric process for total Palladium estimation and application for live cell imaging

Anup Kumar Bhanja, Snehasis Mishra, Ketaki Kar, Kaushik Naskar, Suvendu Maity, Krishna Das Saha, Chittaranjan Sinha*

Fig S1: Powder X-ray diffraction pattern of RD-2.

Fig.S2. FT-IR spectrum of RD-2 in KBr disc

Fig.S3. ^{1}HNMR spectrum of RD-2 in $CDCl_3$

Fig.S4. 13CNMR spectrum of RD-2 in $CDCl_3$

Fig.S5. Mass spectrum of RD-2

Fig.S6. Fluorescence intensity changes profiles of 100 μM RD-2 in CH_3CN–water (HEPES buffer, pH =7.4; v/v, 1/4) in presence of selected metal ions at excitation wavelength 505 nm.

Fig.S7. The linear dynamic response of RD-2 for Pd^{2+} and the determination of the detection limit (LOD) for Pd^{2+} .

Fig.S8. Plausible mechanism of Pd^{2+} induced spirolactam ring opening and fluorescece emission change strategy of probe(our previous report).

Fig.S9. Mass spectrum of RD-2 with Pd^{2+}.

Fig.S10. ^{1}HNMR spectrum (300MHz) of RD-2 in CD_3CN with Pd^{2+}.

Fig.S11. FT-IR spectrum of RD-2 in KBr disc with Pd^{2+}.

Fig.S12. ^{13}C NMR spectrum of RD-2 in CD_3CN-$CDCl_3$ with Pd^{2+}.

Fig.S13. Effect of pH on the fluorescence activity of RD and RD with Pd^{2+} in (CH_3CN/H_20, ¼, v/v, HEPES buffer).

Table S1. Comparative information of different probes for detection of Pd^{2+} and their LOD and Reference.

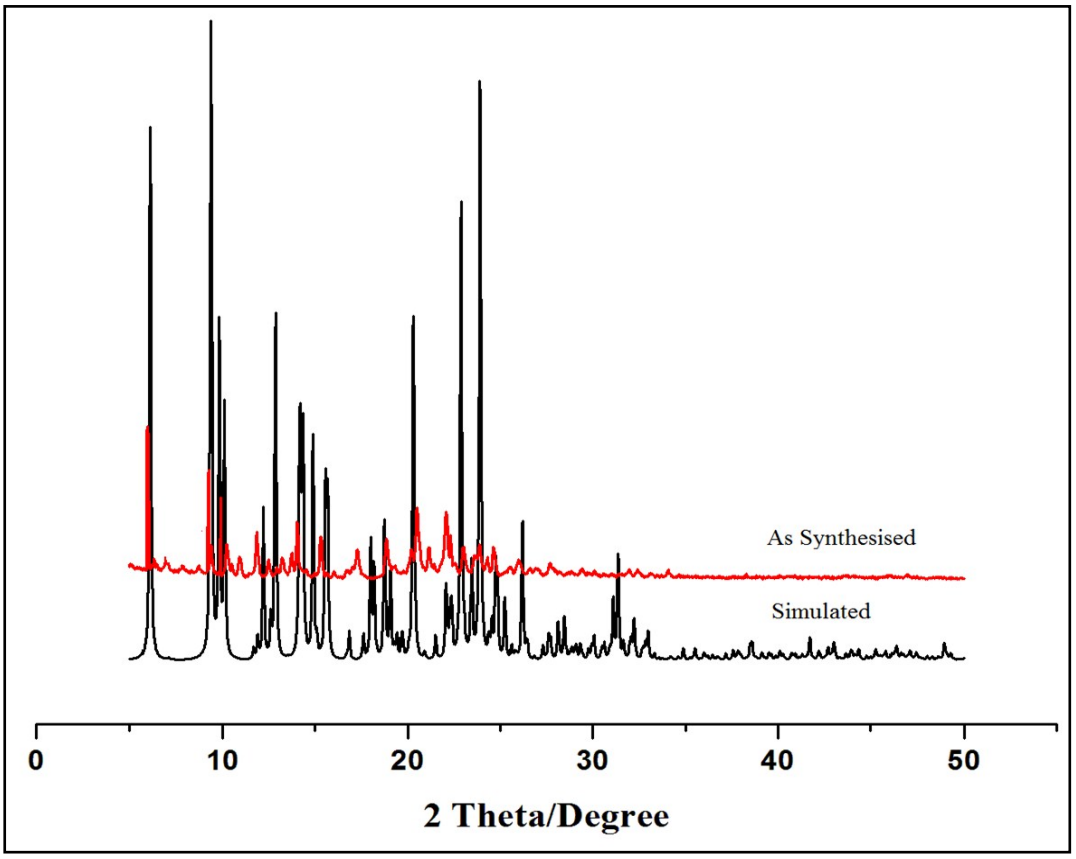

Fig S1: Powder X-ray diffraction pattern of RD-2.

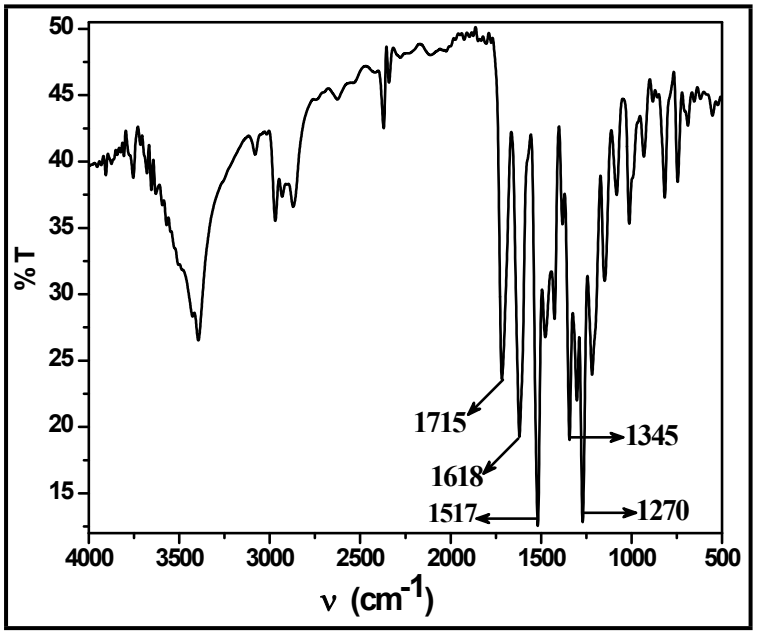

Fig. S2. FT-IR spectrum of RD-2 in KBr disc.

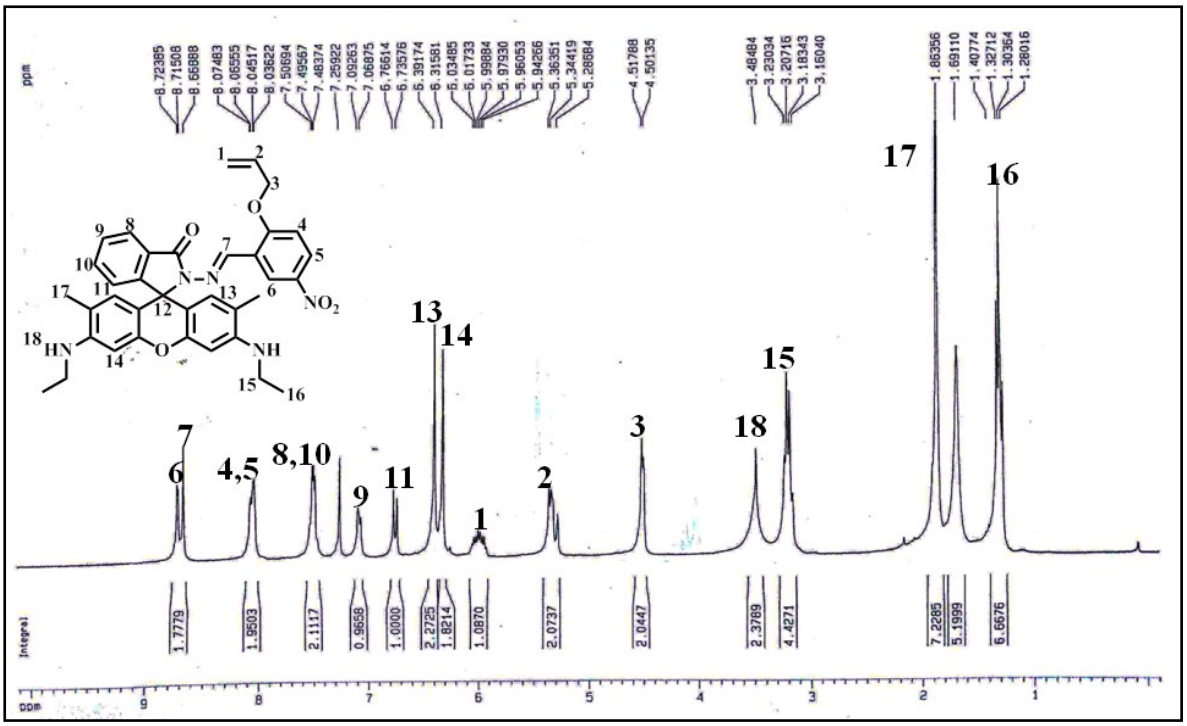

Fig. S3. [1]HNMR spectrum(300MHz) of RD-2 in $CDCl_3$.

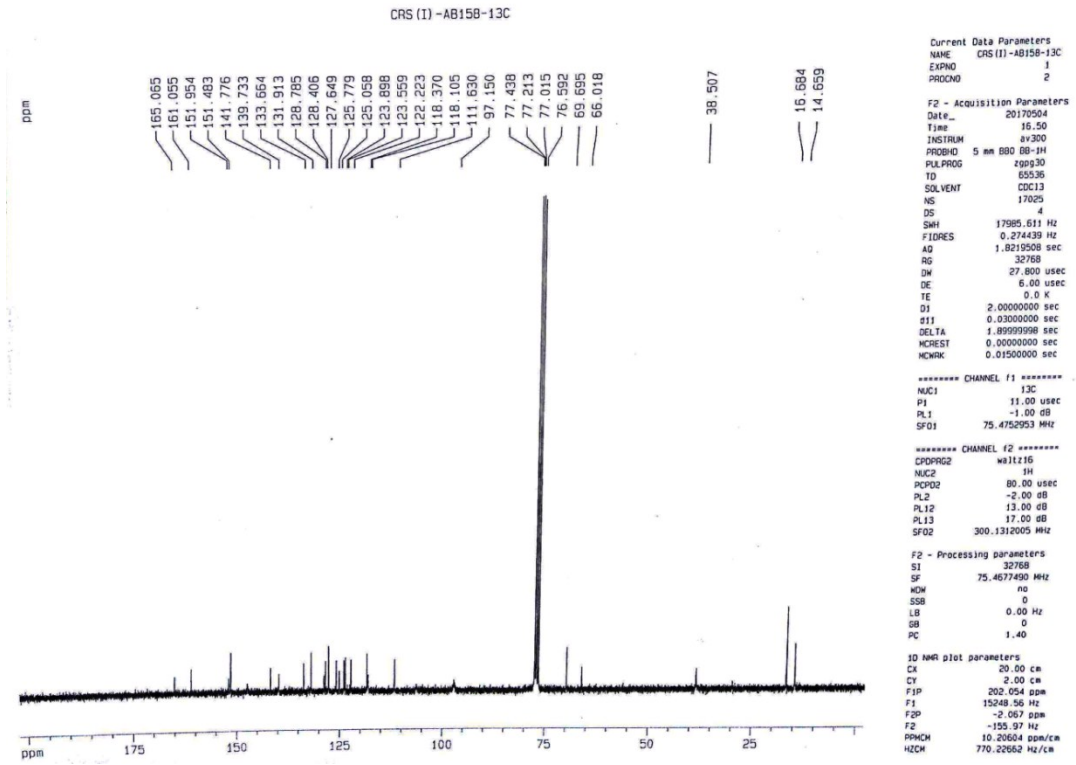

Fig. S4. [13]CNMR spectrum of RD-2 in $CDCl_3$

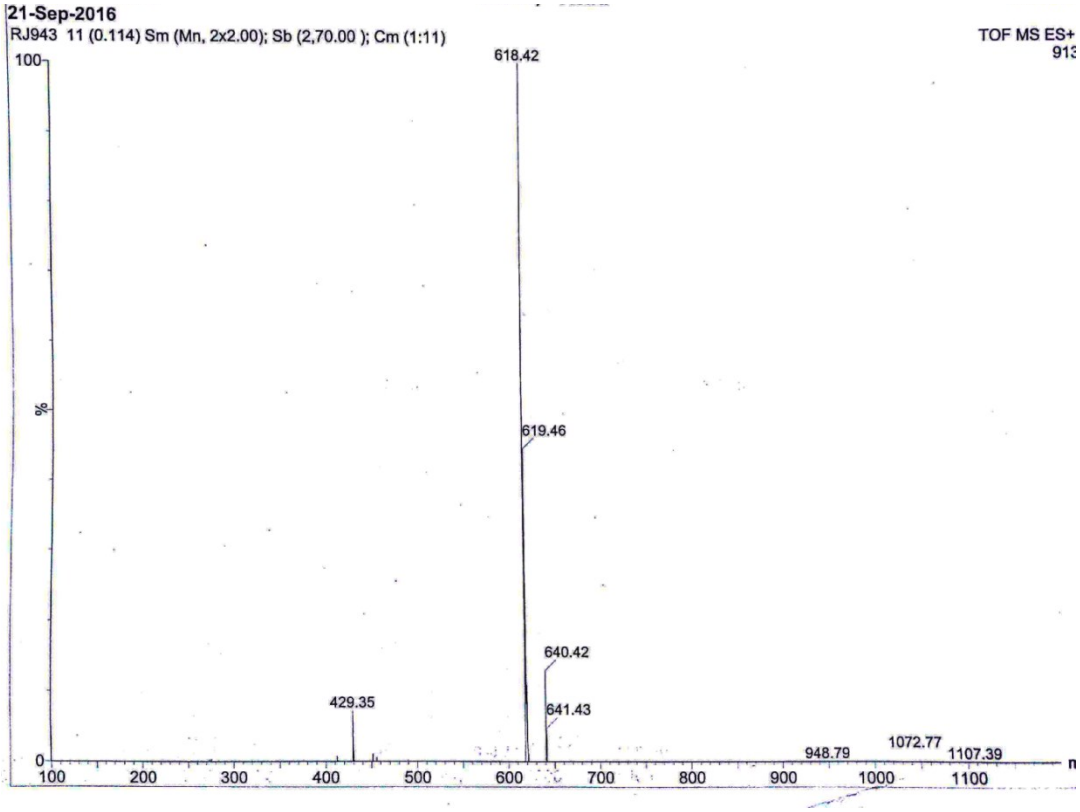

Fig. S5. Mass spectrum of RD-2.

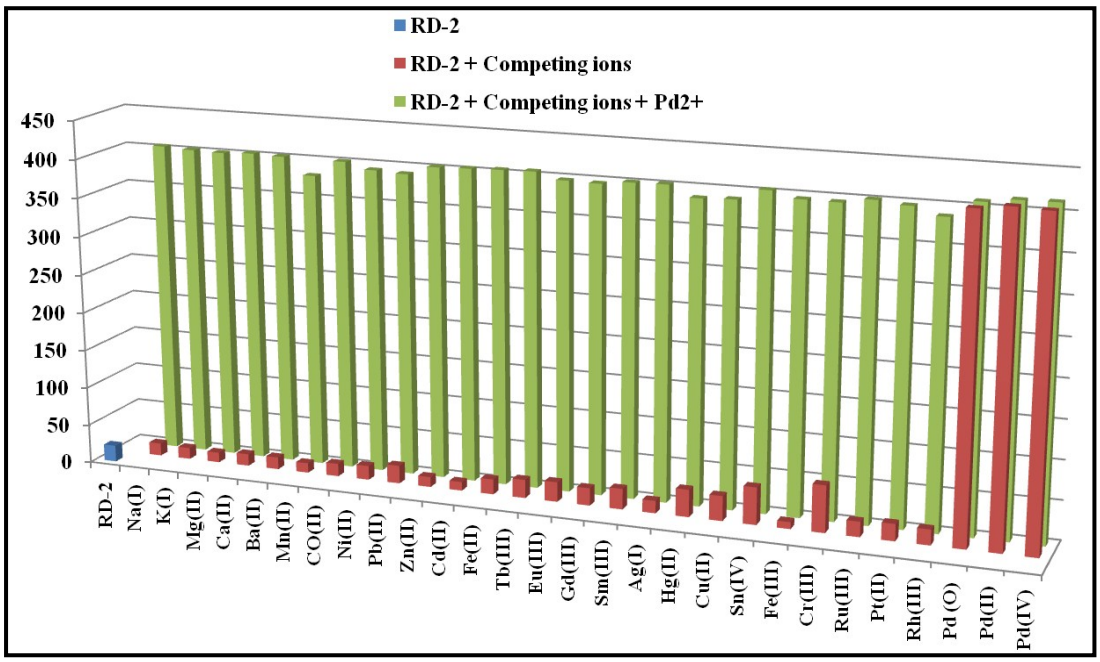

Fig. S6. Fluorescence intensity changes profiles of 100 μM RD-2 in CH_3CN–water (HEPES buffer, pH =7.4; v/v, 1/4) in presence of selected metal ions at excitation wavelength 505 nm.

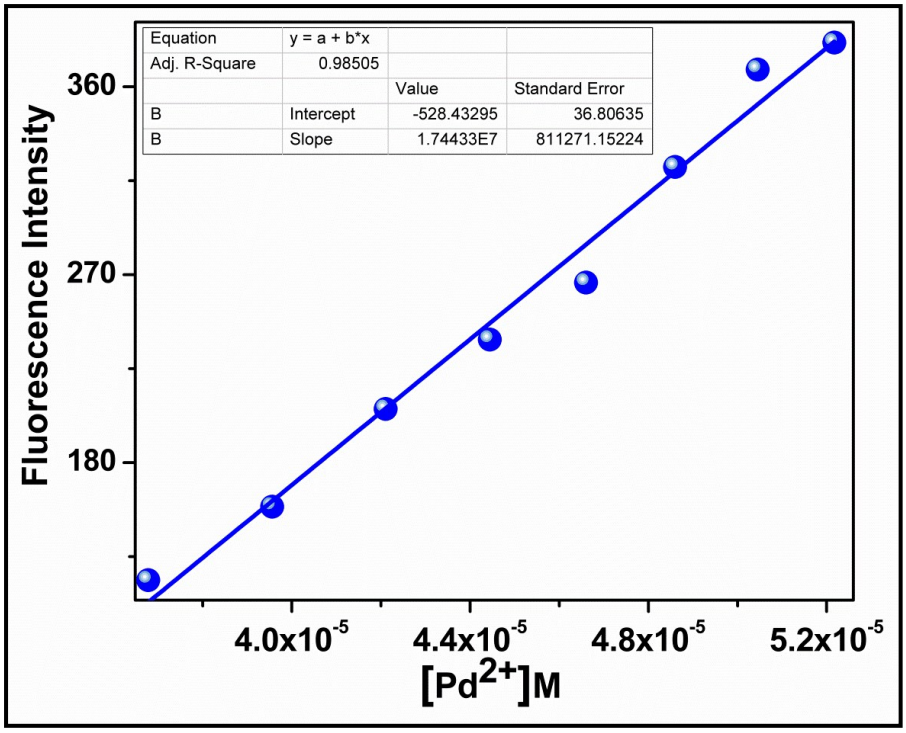

Fig. S7. The linear dynamic response of RD-2 for Pd^{2+} and the determination of the detection limit (LOD) for Pd^{2+}.

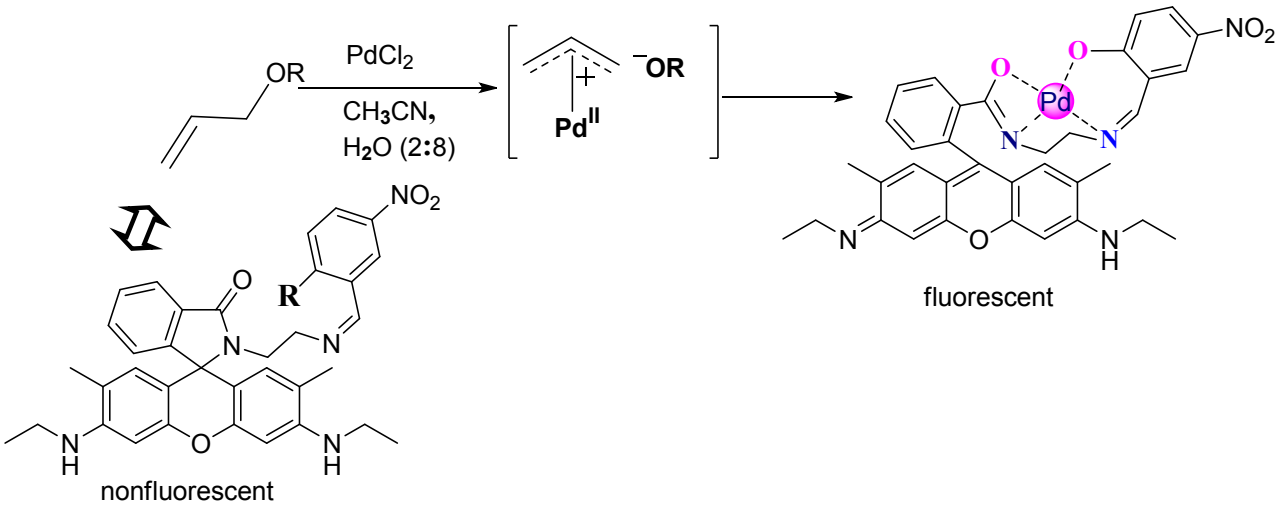

Fig. S8. Plausible mechanism of Pd^{2+} induced spirolactam ring opening and fluorescece emission change strategy of probe(our previous report).

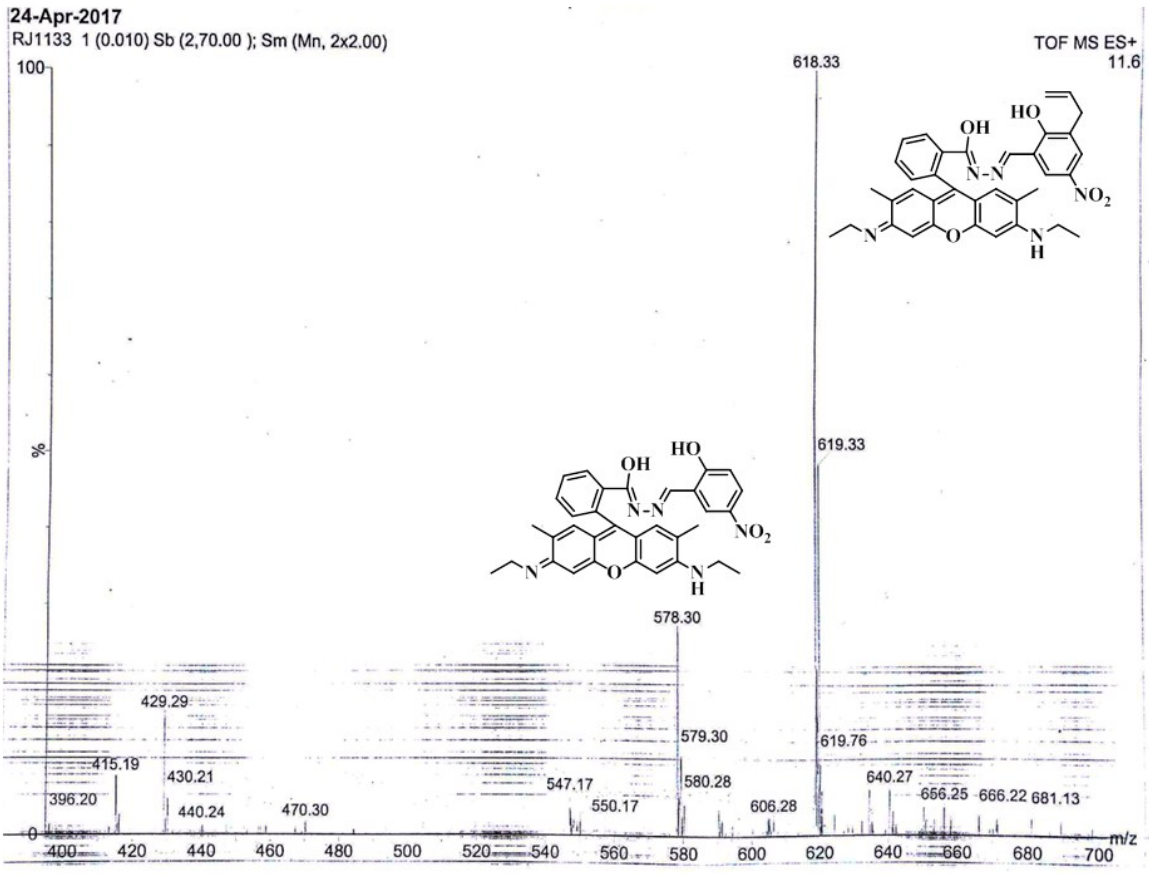

Fig. S9. Mass spectrum of RD-2 with Pd^{2+}.

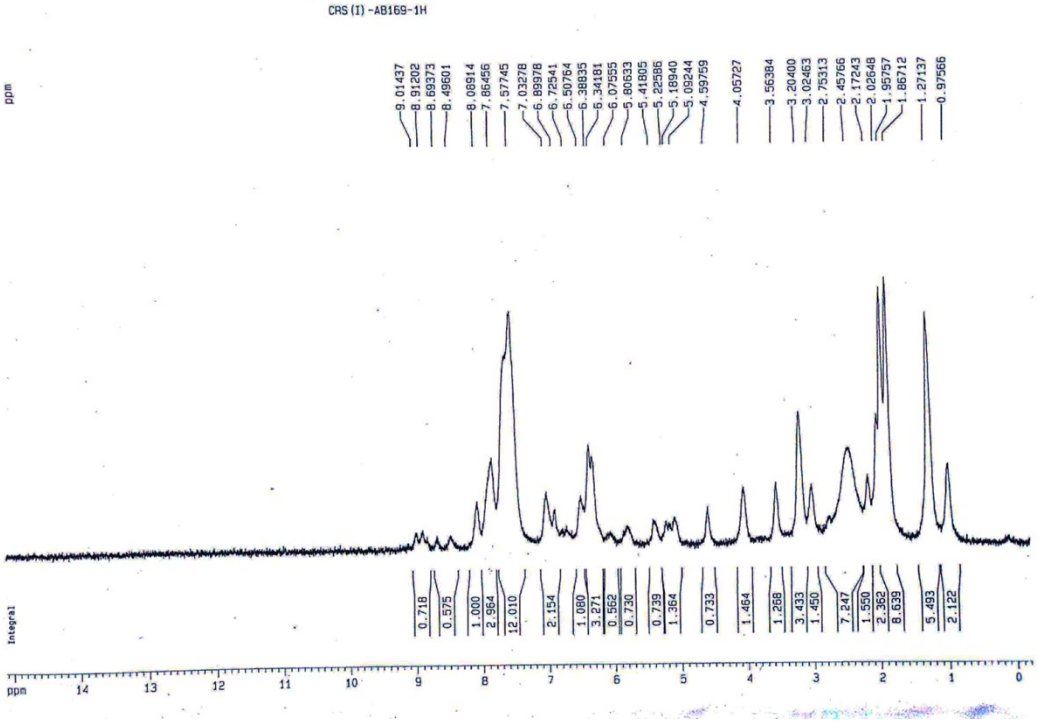

Fig. S10. ^{1}HNMR spectrum (300MHz) of RD-2 in CD_3CN with Pd^{2+}.

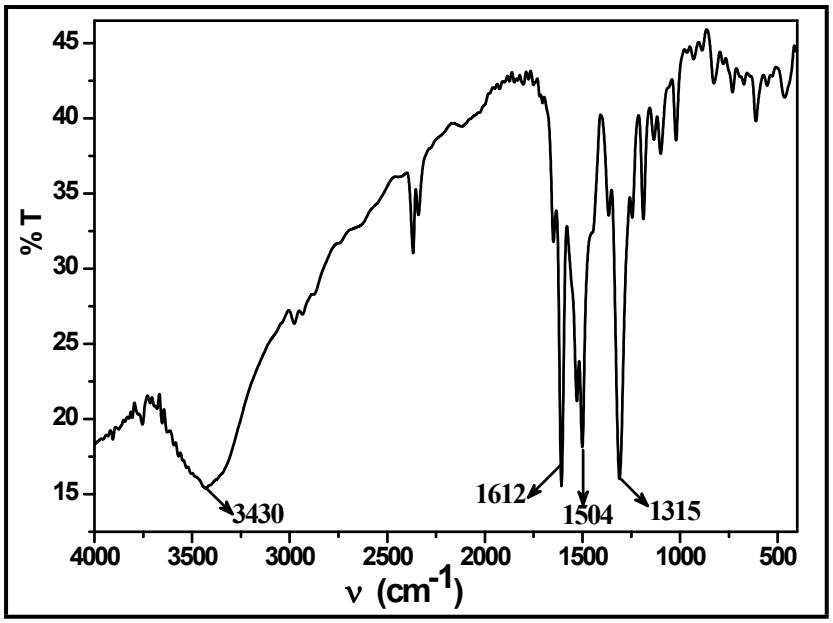

Fig. S11. FT-IR spectrum of RD-2 in KBr disc with Pd^{2+}.

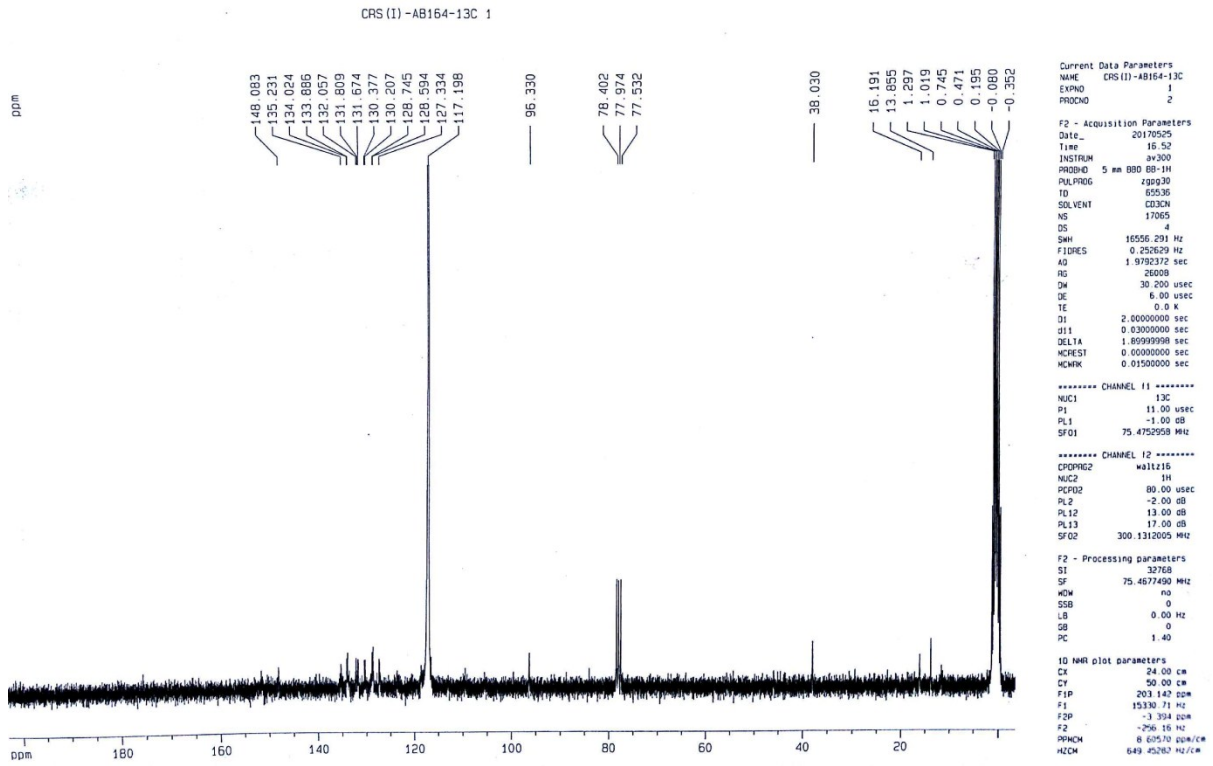

Fig. S12. ^{13}C NMR spectrum of RD-2 in CD_3CN-$CDCl_3$ with Pd^{2+}.

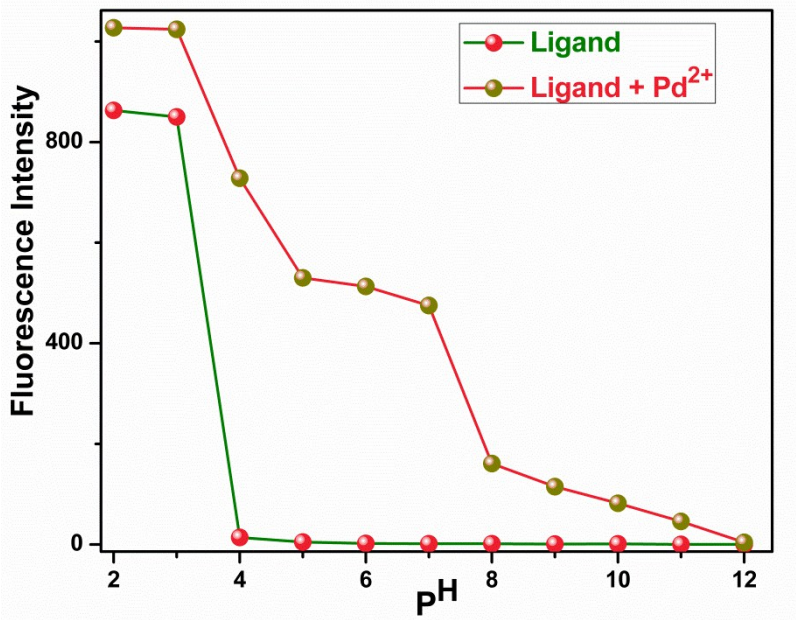

Fig. S13. Effect of pH on the fluorescence activity of RD-2 and RD-2 with Pd^{2+} in (CH_3CN/H_20, ¼, v/v, HEPES buffer).

Table S1. Comparative information of different probes for detection of Pd^{2+} and their LOD and Reference

Sl.No.	Fluorophore	LOD, nM	Ref.
1.	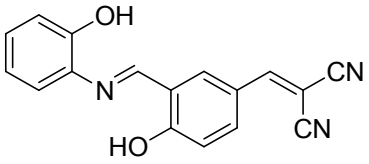	100	33
2.	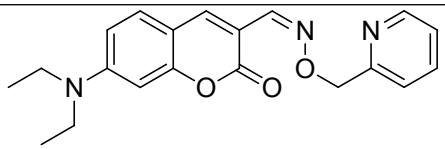	55	34
3.	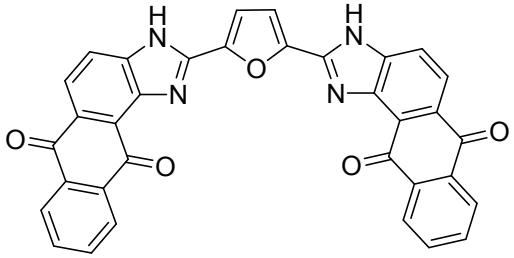	1650	35

4.	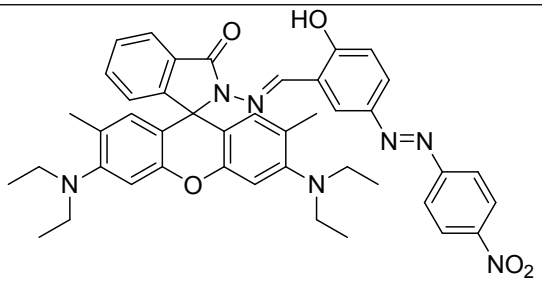	450	36
5.	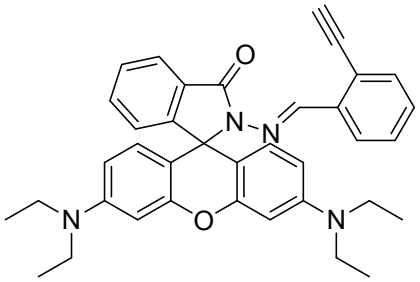	191	37
6.	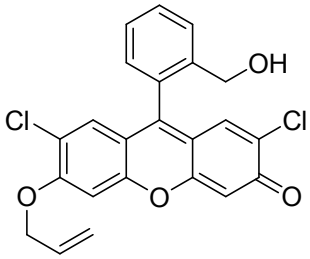	3900	38
7.	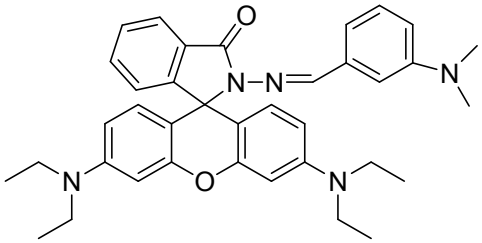	280	39
8.	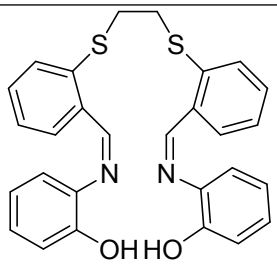	120	40

9.	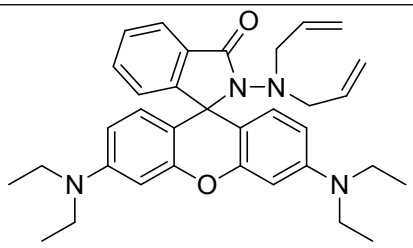	185	41
10.	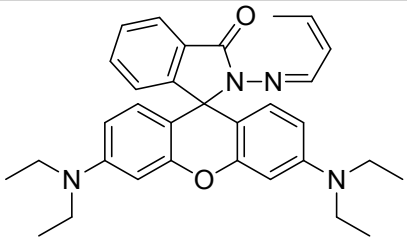	190	42
11.	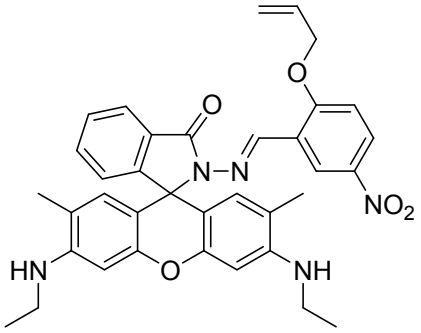	95	This Work